



Fig. S1 Schematic diagram of semi-enclosed inner tube.

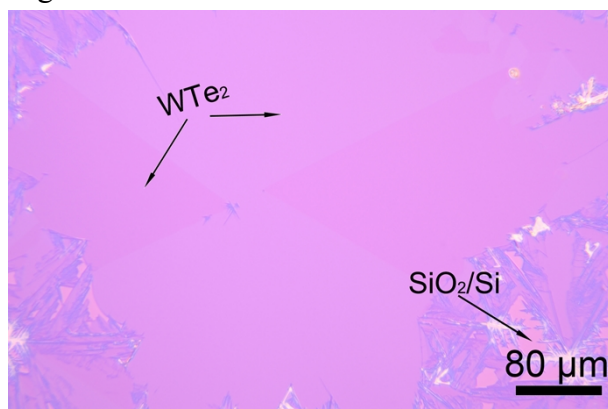


Fig. S2 Optical microscope image of the large-area WTe_2 in region III.

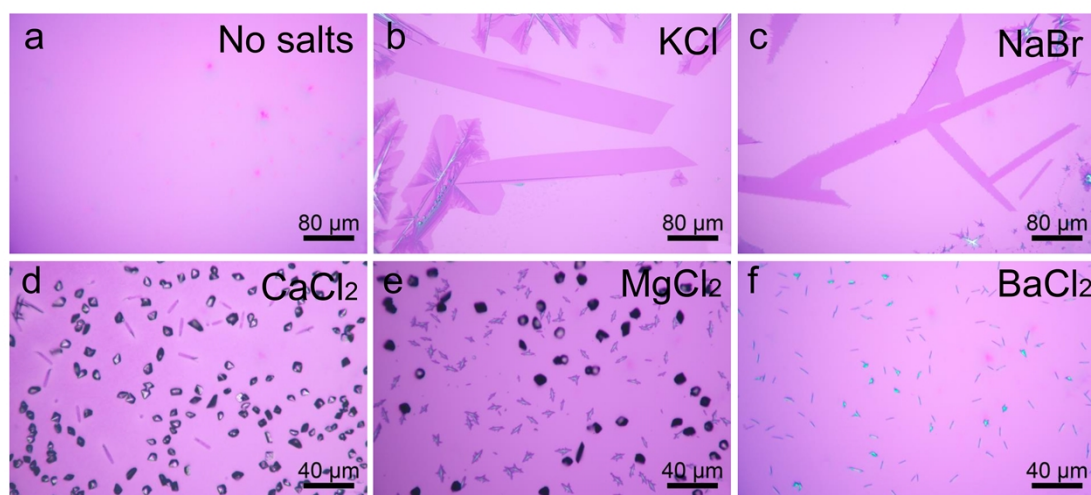


Fig. S3 Optical microscope images of the prepared WTe_2 , using WO_3 precursor a) alone and with fluxing agents of b) KCl , c) NaBr , d) CaCl_2 , e) MgCl_2 and f) BaCl_2 .

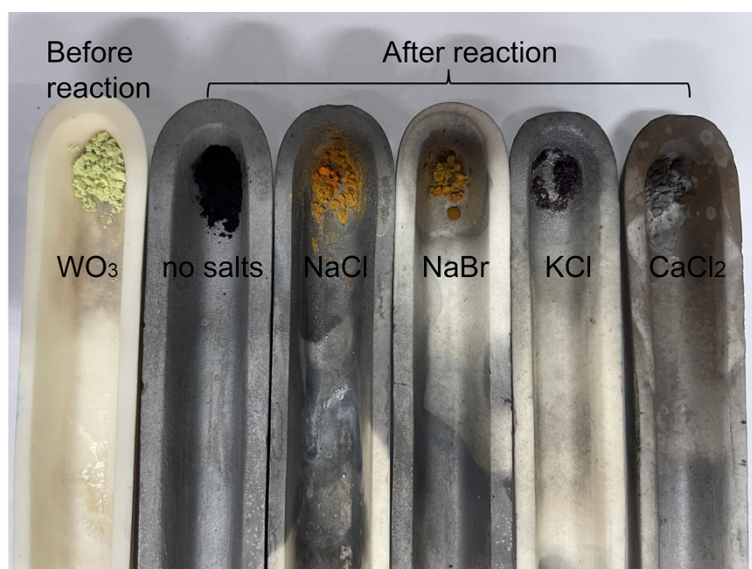


Fig. S4 W source before and after reaction.

To demonstrate the role of NaCl in the growth process, we have also conducted comparative experiments using WO_3 precursor without salt and with other types of salts such as KCl, NaBr, CaCl_2 , MgCl_2 and BaCl_2 . According to the experimental results in Fig. S3, we found that the use of KCl and NaBr facilitates the growth of large-area WTe_2 in a manner similar with NaCl. Conversely, CaCl_2 , MgCl_2 , and BaCl_2 only lower the melting point of WO_3 without promoting the growth of WTe_2 . This indicates that alkali metal ions have a catalytic effect on the growth of TMDs materials, while alkaline earth metals ions do not. The W source after reaction is shown in Fig. S4. We can see that the WO_3 without salt assist only changes color from yellow to black after the reaction without any reduction in volume. In contrast, the salt-assisted WO_3 shows a clear molten state and reduces in volume. This indicates that the addition of salt lowers the melting point of WO_3 .

We take NaCl as an example, the first step of molten-assisted WTe_2 synthesis can be as follows:



The melting point of $\text{WClO}_4/\text{WO}_2\text{Cl}_2$ is much lower than that of WO_3 . In terms of the reaction process (1), the salt not only can lower the melting point of the W source precursor, but also forms molten salt ($\text{Na}_2\text{WO}_4/\text{Na}_2\text{W}_2\text{O}_7$) and leads to a liquid-gas growth of WTe_2 . According to the previous reports,^[1,2,3] alkali metal halides rather than alkaline earth metal halides were also verified to be beneficial for the growth of 2D materials. Similar to molten salts intercalate into the interlayer space of Transition-Metal Nitrides,^[R1] in this work, $\text{Na}_2\text{WO}_4/\text{Na}_2\text{W}_2\text{O}_7$ also has the effect of reducing the activation energy of (110) facet and promoting the large area growth of WTe_2 film.

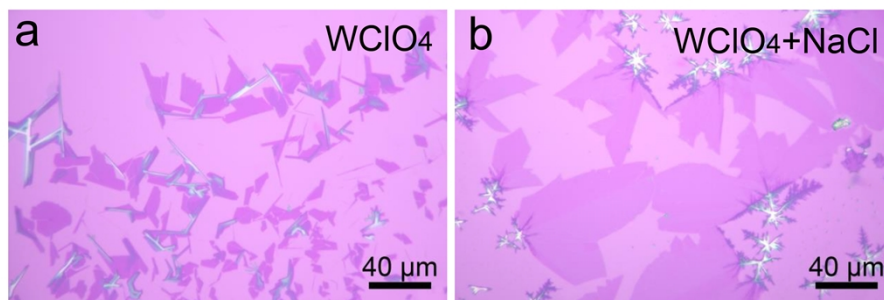


Fig. S5 Optical microscope images of WTe_2 , using WClO_4 as precursor a) without salt-assist and b) with NaCl fluxing agent.

As shown in the Fig. S5 a, WTe_2 samples can be grown using WClO_4 as the W source without additional salts, but the growth parameters still need to be adjusted. We performed a control experiment under the same growth parameters, and added 15 mg of NaCl to the WClO_4 precursor. Compared to the experiment without NaCl , the samples grown with 15 mg of NaCl added to the WClO_4 precursor have thinner thickness and larger size (Fig. S5b). As shown in Fig. S3a, no samples are obtained on the substrate, when using only WO_3 and Te as precursors. The results indicate that the addition of NaCl not only lowers the melting point of the W source precursor, but also has a catalytic effect on the growth of WTe_2 .

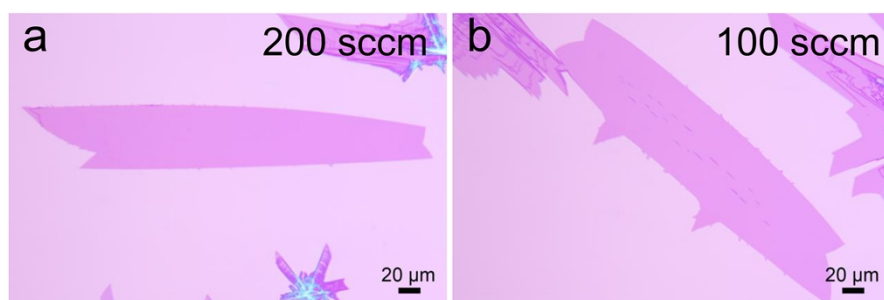


Fig. S6 Optical microscope images of WTe_2 , when the gas flow rate is a) 200 sccm and b) 100 sccm, respectively.

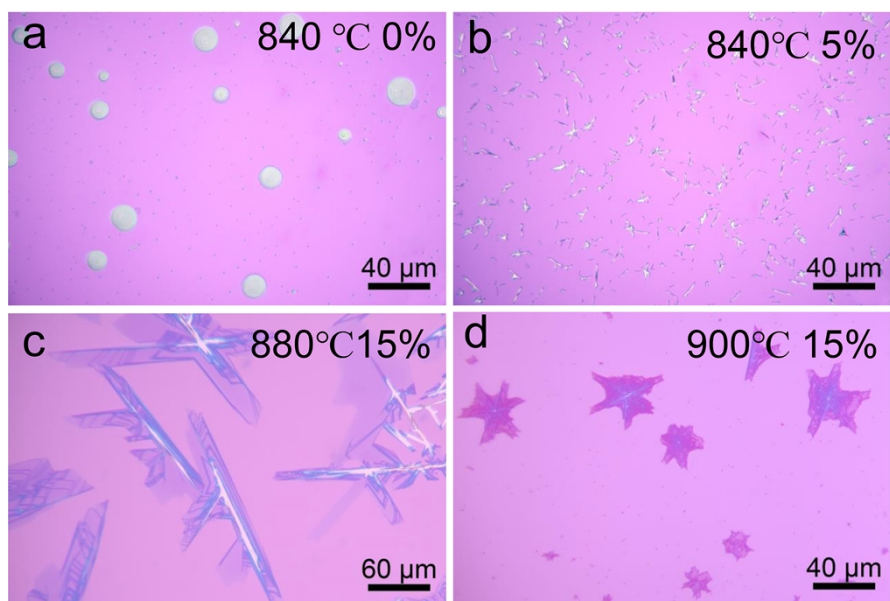


Fig.S7 Optical microscope images of WTe_2 growing using the reaction parameters of (a) 0% and (b) 5% H_2 concentration under 840 °C, (c) 880 °C and (d) 900 °C under 15% H_2 concentration.

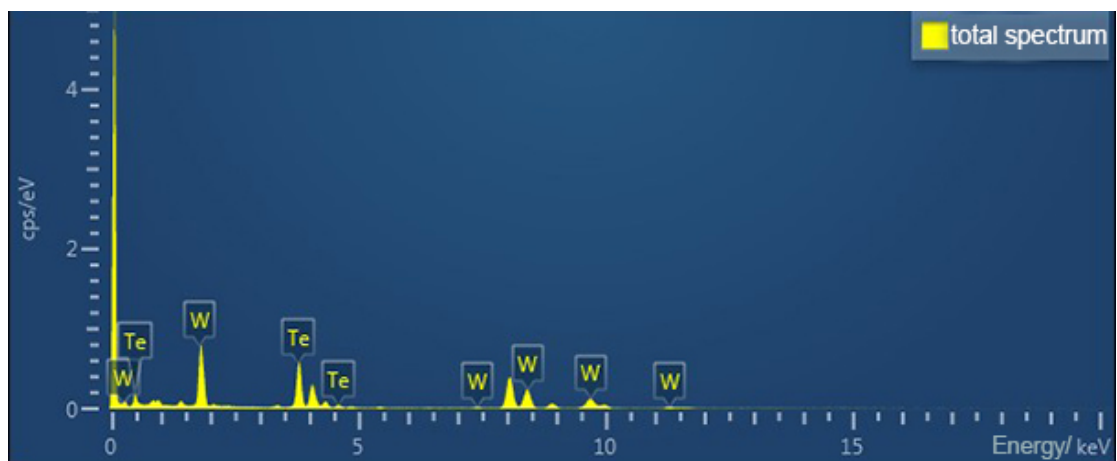


Fig.S8 Elemental analysis of the transferred sample by EDS.

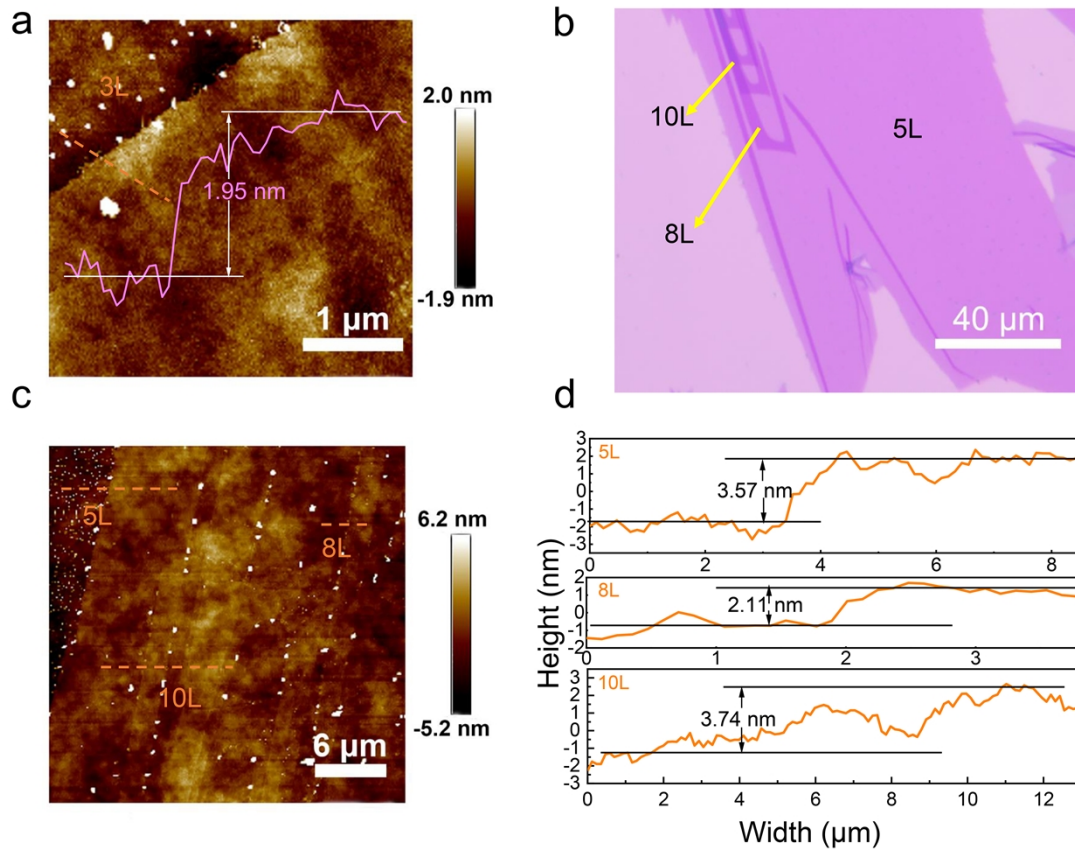


Fig. S9 a, c, d) AFM characterization results of 3L, 5L, 8L, 10L WTe₂ and b) Optical microscope images of 5L,8L,10L.

Fig. S9 b is a partial enlargement of Fig. 4a. From Fig. S9 b, we can see that the WTe₂ is grown layer by layer. We can first distinguish the difference in sample thickness from the color. The thicker the sample, the darker the color. We labeled the 5L, 8L, and 10L samples in Fig. 4a. From AFM measurements, we determined the specific thicknesses of the 5L is 3.57nm. From Fig.4a, we can see that the 5L sample has a large size, while 8L and 10L samples have smaller sizes and are stacked on top of the 5L sample. Therefore, the thickness of the 8L sample is 5.68 nm, calculated as $3.57 \text{ nm} + 2.11 \text{ nm} = 5.68 \text{ nm}$. The thickness of the 10L sample is 7.31 nm ($3.57 \text{ nm} + 3.74 \text{ nm} = 7.31 \text{ nm}$).

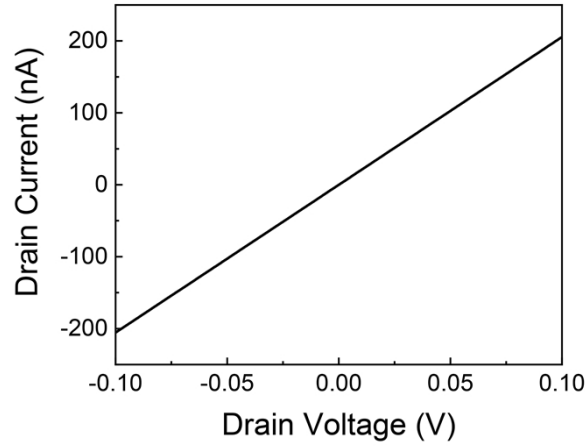


Fig. S10 I - V curve of WTe_2 device.

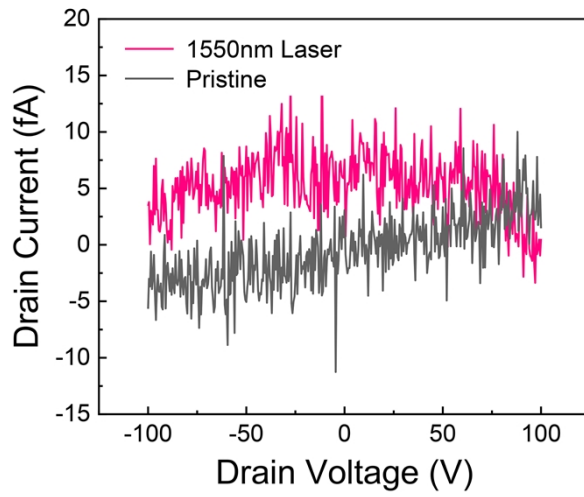


Fig. S11 I_{ds} - V_{ds} output curves of the 285nm SiO_2/Si under 1550nm laser.

Table S1. Summary of photodetectors based on 2D semimetal materials

No.	Material	Responsivity ($mA W^{-1}$)	Wavelength (nm)	Test temp.(K)	Ref.
1	Graphene	230	1550	300	[4]
2	Td-MoTe ₂	0.07	1550	300	[5]
3	Cd3As ₂	12.48	450-10600	300	[6]
4	TaIrTe ₄	0.02	532-10600	300	[7]
5	TaIrTe ₄	0.03013	1550	300	[8]

		130.2	4000	300	[8]
6	Td-WTe ₂	2.5×10 ⁵	3800	77	[9]
7	1T'-WTe ₂	118	1500	300	This work
		408	2700	300	This work

S1. The specific detectivity (D^*) can be calculated by the following equation:

$$D^* (\text{Jones}) = \frac{RA^{1/2}}{(2eI_{\text{dark}})^{1/2}}$$

Where R is the photoresponsivity, A is the area of the device, e is the elementary charge, and I_{dark} is the dark current. We could obtain a D^* ranging from 10^5 to 10^6 Jones at all tested powers.

Reference

- [1] H. Jin, Q. Gu, B. Chen, C. Tang, Y. Zheng, H. Zhang, M. Jaroniec, S. Qiao, *Chem*, 2020, 6, 2382-2394.
- [2] M. Kim., M. Son, D. Seo, J. Kim, M. Jang, D. Kim, S. Lee, S. Yim, W. Song, S. Myung, J. Yoo, S. Lee, K. An, *Small*, 2023, 2206350.
- [3] K. Chen, Z. Chen, X. Wan, Z. Zheng, F. Xie, W. Chen, X. Gui, H. Chen, W. Xie, Xu, J. *Adv. Mater.*, 2017, 29, 1700704.
- [4] Z. Chen, Z. Cheng, J. Wang, W. Xi, J. Xu, *Adv. Opt. Mater.*, 2015, 3, 1207-1214.
- [15] J. Lai, X. Liu, J. Q. Wang, K. Zhang, X. Ren, Y. Liu, Q. Gu, X. Zhou, W. Lu, Y. Wu, Y. Li, J. Feng, S. Zhou, J. Chen, D. Sun, *Adv. Mater.*, 2018, 30, 1707152.
- [6] M. Yang, J. Wang, J. Han, J. Ling, C. Ji, X. Kong, X. Liu, Z. Huang, J. Gou, Z. Liu, F. Xiu, Y. Jiang, *ACS Photonics*, 2018, 5, 3438-3445.
- [7] J. Lai, Y. Liu, J. Ma, X. Zhuo, Y. Peng, W. Lu, Z. Liu, J. Chen, D. Sun, *ACS nano*, 2018, 12, 4055-4061.
- [8] J. Ma, Q. Gu, Y. Liu, J. Lai, P. Yu, X. Zhuo, Z. Liu, J. Chen, J. Feng, D. Sun, *Nat. Mater.*, 2019, 18, 476-481.
- [9] W. Zhou, J. Chen, H. Gao, T. Hu, S. Ruan, A. Stroppa, W. Ren, *Adv. Mater.*, 2019, 31(5): 1804629.